

FATE: Far Tail Explorer

Lead: Masatoshi Yamauchi

Swedish Institute of Space Physics (IRF), Box 812, S-98128 Kiruna, Sweden

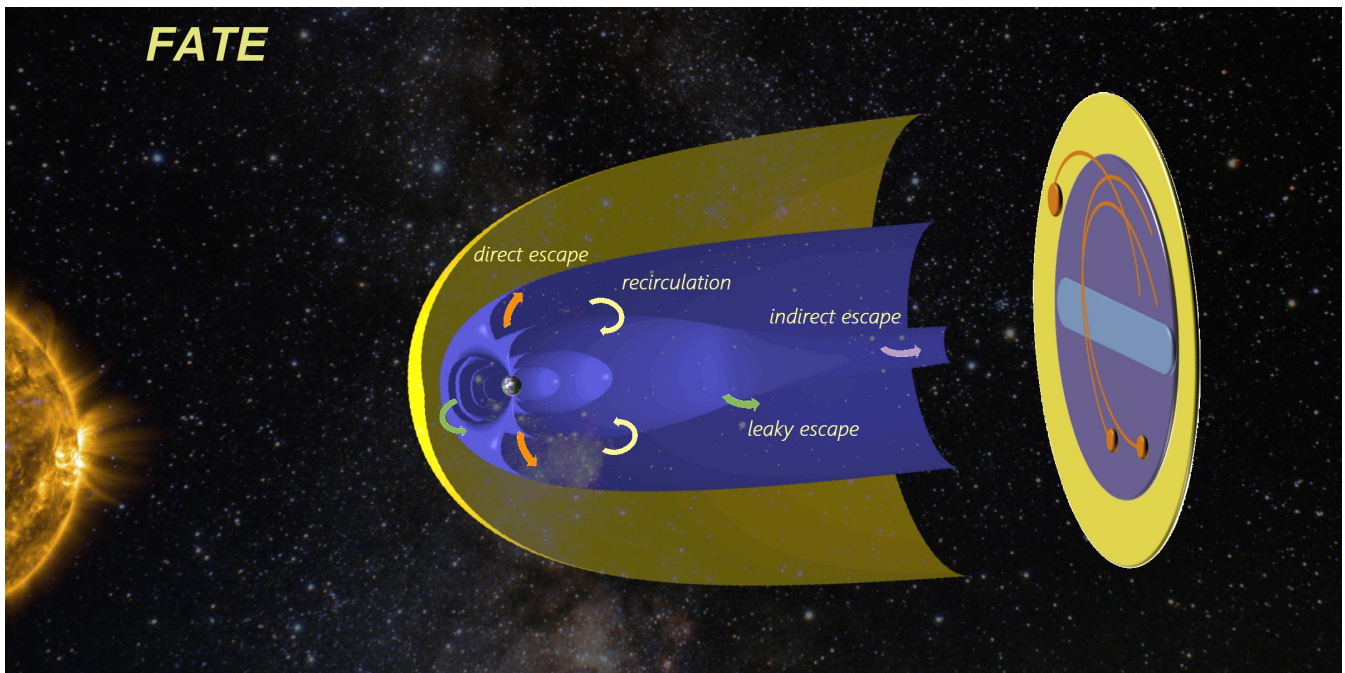
E-mail: M.Yamauchi@irf.se, Phone: +46-980-79120, Fax: 046-980-79050

Co-Lead: Johan De Keyser

Royal Belgian Institute for Space Aeronomy (BIRA-IASB),

Ringlaan 3, B-1180 Brussels, Belgium

E-mail: johandk@aeronomie.be, Phone: +32-2-3730368, Fax: +32-2-3748423



Theme

Non-thermal ion escape: amount, composition, variability, and escape routes.

Aim

The FATE mission aims to obtain the total flux, composition, and variability of escaping terrestrial ions from L2, the ultimate downstream position, for different solar, solar wind and geomagnetic conditions. This requires measurement of the flux, composition, and energies of the escaping ions across the magnetotail cross-section, as well as determining the area of the different regions in the tail corresponding to the major escape mechanisms, as a function of external conditions. Therefore, the following sub-themes must be addressed:

- (1) Flux and active size measurements for principal ions far downstream with velocity from nearly zero to the solar wind speed (as high as 800 km/s) as a function of geomagnetic, solar and solar wind conditions.
- (2) Transient interaction between magnetosphere and interplanetary shocks / magnetic clouds / solar energetic particles (SEP) and its effect on ion escape, by comparing L1 and L2 monitor data.
- (3) Identification of the relative importance of the different ion escape routes and mixing of different plasmas far downstream.

The solar conditions, the solar wind at L1, and the terrestrial conditions will be continuously monitored by the Space Weather (SWE) programs of ESA SSA and NOAA, while relevant geomagnetic indices are always available from the World Data System.

Mission summary

One main spacecraft and two identical sub-spacecraft (a 6U cubesat form factor is considered) following Lissajous or Halo orbit around L2 scan the Earth's magnetotail cross-section and measure particles and fields. The nominal operation duration is 6 months.

Core Hardware Team Members (PIs, co-PIs, and lead-CoIs):

| (1) Particle consortium (main spacecraft), Consortium PI: I. Dandouras | | | | |
|--|-------------------------------|------------------------------------|----------------------|------------------|
| instrument | name | organization | country | funding |
| co-PI for ion mass < 40 keV | I. Dandouras | IRAP, Toulouse | France | CNES |
| co-PI for ion energy 0.1-60 keV | M. Wieser | IRF, Kiruna | Sweden | SNSA |
| co-PI/coI for ion 30-150 keV | A. Millio | IAPS, Rome | Italy | ASI |
| co-PI for cold ion mass/isotope | P. Wurz | U. Bern | Switzerland | SSO |
| co-PI for electron | A. Fazakerley | MSSL | UK | UKSA |
| co-PI for energetic particles (EP) | M. Dunlop | RAL Space, Didcot | UK | UKSA |
| co-PI for EP signal process system | L. Kistler | U. New Hampshire | USA | NASA |
| co-PI for particle DPU | J. Martin-Torres | LTU, Luleå | Sweden + New Zealand | |
| (2) Field consortium (main spacecraft) / Space Environment Model, Consortium PI: J. De Keyser | | | | |
| co-PI for magnetometer | R. Nakamura | IWF, Graz | Austria | ALR/FFG |
| coI for magnetometer | J. Eastwood | IC, London | UK | UKSA |
| co-PI for Langmuir probe (LP) | M. Morooka | IRF, Uppsala | Sweden | SNSA |
| coI for LP | J. De Keyser | BIRA-IASB, Brussels | Belgium | BELSPO |
| co-PI for Frequency analyzer | B. Grison | IAP, Prague | Czech | PRODEX |
| (3) Sub-spacecraft and related system in main spacecraft, Consortium PI: E. Kallio | | | | |
| co-PI for cubesat bus | R. Funase | U. Tokyo, Hongo | Japan | JAXA |
| co-PI for cubesat bus | E. Kallio | Aalto U., Espoo | Finland | Business Finland |
| co-PI for deployment & transmissions | M.R. Emami | LTU, Kiruna | Sweden | SNSA |
| co-PI for ion < 15 keV | M. Wieser | same as above | Sweden | SNSA |
| coI for ion < 15 keV | E. Vilenius | MPS, Göttingen | Germany | |
| co-PI for ion 15-120 keV | A. Poppe | SSL, Berkeley | USA | NASA |
| coI for ion 15-120 keV | J.H. Seon | Kyug Hee U. | S. Korea | |
| co-PI/coI for magnetometer | N. Ivchenko or R. Nakamura | KTH, Stockholm same as above | Sweden Austria | SNSA ALR/FFG |
| co-PI for LP (TBD) | J. De Keyser | same as above | Belgium | BELSPO |
| (4) UV imager (TBD) PI: E. Quemerais | | | | |
| co-PI for UV imager | I. Yoshikawa | LATMOS, Paris U. Tokyo, Kashiwa | France Japan | CNES JAXA |

The abbreviations are:

IRF: Swedish Institute of Space Physics

IRAP: CNRS and Paul Sabatier Toulouse University, Institut de Recherche en Astrophysique et Planétologie

MSSL: Mullard Space Science Laboratory, University College London

RAL: RAL Space, Rutherford Appleton Laboratory, Science and Technology Facilities Council

IAPS: INAF/Istituto di Astrofisica e Planetologia Spaziali

BIRA-IASB: Royal Belgian Institute for Space Aeronomy

IWF: Institut für Weltraumforschung

IC: Imperial College

IAP: Institute of Atmospheric Physics, Academy of Sciences

KTH: Royal Institute of Technology

LTU: Lulea University of Technology

MPS: Max Planck Institute for Solar System Research

SSL: University of California Berkeley, Space Science Laboratory

LATMOS: Laboratoire Atmosphères Milieux Observations Spatiales

(Key Science members from the other affiliations)

O. Marghita (Institute of Space Science, Bucharest, Romania), S. Haaland (U. Bergen, Norway), J. Borovsky (Space Science Institute, Boulder, USA), M. Hirahara (Nagoya University, Japan), R. Slapak (EISCAT Scientific Association, Sweden), Y. Saito (ISAS, Japan).

1. Scientific goal of the mission

Evolution of the Earth's atmosphere is a key science theme. Mars and Venus developed atmospheres that are markedly different from that of Earth, of which the atmosphere evolved in conjunction with the appearance of life. While the geological record gives insight in surface-atmosphere gas exchanges, atmospheric evolution can never be understood without a proper assessment of the importance of atmospheric escape. While the current neutral escape from the Earth's atmosphere is reasonably characterized to be small, the ion escape is more complicated because of the diversity of escape mechanisms, the complexity of ion escape routes, and the strong time variability of the phenomena. The FATE mission therefore addresses the science question **"What is the non-thermal ion escape rate from Earth as a function of solar, solar wind, magnetospheric, and upper atmospheric conditions?"** This question is directly related to Cosmic Vision theme #2 "How does the Solar System work?" and indirectly contributes to Cosmic Vision theme #1 "What are the conditions for planet formation and the emergence of life?"

1.1. Significance of the ion escape

Past space-based studies of Mars (Phobos-2, Mars Express, MAVEN), Venus (Venus Express), and Titan (Cassini) show that all unmagnetized planets/moons with an atmosphere are losing their atmosphere by non-thermal mechanisms with an ion loss rate of 10^{-2} - 10^0 kg/s on average. For the Earth, a magnetized planet, satellite observations (DE-1, Akebono, FAST, Polar, Cluster) show that the ion outflow rate from the ionosphere is higher by 1-2 orders of magnitude, at a level of 10^0 - 10^2 kg/s depending on the geomagnetic, solar, and solar wind conditions. If all of these ions escape, the ion escape rate is large enough to have played a major role in the past evolution of the Earth's atmosphere and even in the evolution of life.

However, it is still unknown how much of these ions ultimately escape into interplanetary space, as some ions may be trapped by the geomagnetic field. Before the Cluster mission, the majority of the outflowing ions were assumed to return as the $J \times B$ force drives them back to Earth, even if they enter the deep magnetotail. This caused the paradigm "*the geomagnetic field protects the atmosphere from escape*". This paradigm, however, is presently being challenged.

Cluster identified three major escape routes, as illustrated on the cover page: (a) a "direct" route in the open part of the geomagnetic field where escaping ions mix into the high-latitude solar wind flow (high-latitude magnetospheric boundary region), (b) a "leaking" route from the inner magnetosphere to the magnetosheath or to the magnetotail (plasmaospheric

plume and ring current particles crossing the magnetopause, plasmaospheric erosion due to storm-time magnetospheric convection), and (c) an "indirect" route through the nightside magnetosphere (plasma sheet and magnetotail) when the Earthward $J \times B$ force is not strong enough to bring back these ions. The amount of ion escape and ion return through these routes, and the net balance, are unknown.

Even considering only the first route, the amount of ion escape may be large enough to affect the past evolution of the biosphere (Slapak *et al.*, 2017, doi:10.5194/angeo-35-721-2017, Figure 7). It is essential to confirm which fraction of these mixing ions escape along this route, as it has been argued that some of them may return after entering the deep magnetotail. The relative importance of the other outflow routes also remains unclear.

In order to assess the total amount of escaping ions, we first have to answer sub-question #1: ***What are the escape fluxes of the principal ions?*** One of the best approaches is to measure the fluxes in the far downstream region, beyond the point of no return. A good place to do this is $> 200 R_E$, where the majority of escaping ions are accelerated to the solar wind speed through ion pick-up and other momentum transfer processes.

1.2. What is missing in past deep tail observations?

So far only ISEE-3 (1983), GEOTAIL (1992-1994), and STEREO-B (2007) approached L2 with ion instruments. Total 9 excursions (GEOTAIL: 6, ISEE-3: 2, STEREO-B: 1) entered deep tail beyond $170 R_E$. However, they were mostly limited to the equatorial region whereas the high-latitude region is more important for ion escape through the direct route. With such orbits, one misses part of the escaping O^+ flux. Also, the instruments used were not suited to the purpose, thus (mis)leading Seki, *et al.* (2001, doi:10.1126/science.1058913) to the above paradigm. In their observations, they distinguished O^+ and H^+ from energy peaks where the two species flow with similar velocities with a cold temperature (i.e., beam-like), and hence their observation was limited to the lobe/mantle region. Also, the upper energy limit was 17 keV without mass separation, i.e., a velocity of 450 km/s for O^+ . Therefore their work missed all O^+ escape during fast solar wind conditions when the O^+ escape flux is known to increase significantly, such as during co-rotation interaction region (CIR) and coronal mass ejection (CME) events, when the solar wind speed normally exceeds 600 km/s (O^+ energy of >30 keV), reaching often 800 km/s (O^+ energy of ~ 60 keV). In such conditions, one can also expect substantial escape of molecular ions (O_2^+ and N_2^+) according to AMPTE and Akebono observations. Therefore, we expect high escaping ion fluxes up to 120 keV during fast solar wind conditions. Escaping

ions at an energy 30 times that of the solar wind H^+ are actually observed at lunar distance by ARTEMIS (Poppe *et al.*, 2016, doi:10.1002/2016GL069715, Figure 1). At that distance, these molecular ions may flow without accompanying atomic ions because of the velocity filter effect.

The GEOTAIL STICS instrument covering 7-230 keV detected both atomic and molecular ions with the O_2^+/O^+ ratio of about 1% in the distant tail (Christon *et al.*, 1994, doi:10.1029/94GL02095). The STEREO-B PLASTIC instrument covering 0.2-80 keV with mass separation capability also found that the O^+ density in the far tail was about 15% of the O^+ density in the near tail as observed by Cluster (Kistler *et al.*, 2010, doi:10.1029/2010GL045075). However, these measurements were again limited to solar minimum and non-storm time.

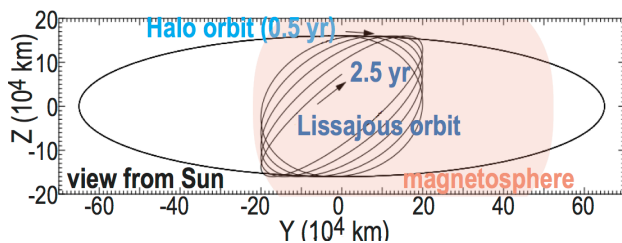


Figure 1: Two types of semi-stable orbit around L2. Different semi-axis diameters can be designed.

1.3. Semi-stable orbit around L2 for 2D coverage

To obtain the total ion loss rate, we need to know the effective cross-section of the high-flux regions, and hence the spatial distribution of the escaping ions in the far tail, beyond which ions may no longer return to Earth. At such distances, the flux distribution is expected to vary by orders of magnitude between different regions. This requires exploration of the full magnetotail cross-section at a constant distance, in order to obtain 2D distributions of the anti-sunward flux of terrestrial ions across the tail. The Sun-Earth L2 Lagrange point satisfies this requirement with its location about $240 R_E$ downstream of the Earth, because semi-stable orbits (Lissajous/Halo orbits as shown in Figure 1) exist for which the spacecraft can move around the L2 saddle point covering both dawn-dusk and north-south directions. With little additional ΔV the spacecraft can easily cover the desired 2D cross-section, which was not possible with the past missions. Staying at the same tailward distance, a two-spacecraft formation is sufficient to separate spatial and temporal variations related to long-duration events such as substorms, rotation of the geomagnetic axis (24 hours), and even a magnetic storm (see §1.4).

L2 is also a good station to monitor the solar wind in addition to L1, because this combination provides higher accuracy in estimating the variation of the solar wind and particularly of Solar Energetic Particles

(SEP) fluxes at Earth. Major solar wind perturbations include CMEs and CIRs, and SEP. SEP, for instance, are either locally produced by interplanetary shocks (front side of CIRs or CMEs) or remotely produced at the solar surface. These two production mechanisms lead to completely different SEP arrival times at Earth. This is particularly important since SEP flux is one of the key parameters that control ion escape. Regardless of these complications, measuring the escape and its spatial distribution solves sub-question #2: **How does the plasma escape respond to transients, including CIRs, CMEs and SEP?**

The various escape routes mentioned above react differently to solar wind variations, and it is essential to be able to disentangle the contribution from different routes. For example, we expect a high content of He^+ from the leaking route. Also, we expect a different N_2^+/O^+ ratio and different energy peak widths for the direct and indirect routes, because different energization efficiencies determine the velocity filter effect and the resultant (interim) destination of outflowing ions. One complication by the observation at L2 is that the contributions of the different escape routes become convoluted along the long trajectory of the particles. Even different plasma regions with clear boundaries near Earth (plasma mantle, plasma sheet, tail lobe, and magnetosheath) can be convoluted because their boundaries are expected to become very disturbed, e.g., by nonlinear evolution of surface waves, with winding of the magnetic field and bifurcation as the distance increases. This problem constitutes sub-question #3: **What is the relative importance of the different ion escape routes?**

At L2 the spacecraft must cover a wide area. According to Cluster observations, a high escape rate is seen on both sides of the magnetopause but not deep inside the magnetosheath toward the bow shock (Slapak *et al.*, 2017). Magnetopause shadowing (leaky escape route) also leads to ion escape just outside the magnetopause. Therefore, in order to cover the 2D cross-section as densely as possible, the spacecraft orbit should not move much beyond the magnetopause into the magnetosheath as there is little escape there. Note also that the magnetosphere is expected to shrink during active periods when we expect a high escape rate. Therefore, we plan to cover the region defined by average (expected) magnetopause size.

The average magnetopause location (from the ARTEMIS statistics) is $27 R_E$ radial distance from the Sun-Earth line at $55 R_E$ downstream, and the radial expansion of the magnetopause is at most hyperbolic with distance, which means an increase from the Moon to L2 ($240 R_E$ downstream) by only a factor of ~ 2 . With solar wind aberration shifting the entire magnetosphere toward dusk by $10\text{-}25 R_E$, the average magnetopause radial distance from the Sun-Earth line

at L2 is about 80 R_E on the dusk side, 40 R_E on the dawn side, and 70 R_E toward north and south. The semi-stable Lissajous/Halo orbits around L2 exist even for much larger radial distances, and all regions of interest are reachable with very small ΔV .

The flux (per unit cross-section) decreases as the effective cross-section of the tailward ion flux region expands. The radial expansion of the escaping ion flux from the ARTEMIS location to L2 is small because the terrestrial ions follow a cycloid motion in the solar wind. This means that the flux of the escaping terrestrial ions decreases slower than the increase of the magnetopause size which is by a factor of ~ 5 from ARTEMIS to L2. GEOTAIL deep-tail observations and ARTEMIS lunar orbit observations of ion flow in the magnetotail and plasma mantle show that the number flux of heavy ions is 2 to 3 orders of magnitude lower than the proton number flux during nominal solar wind condition, with $10^{5-6} \text{ cm}^{-2}\text{s}^{-1}$ for ARTEMIS (Poppe et al., 2016, doi:10.1002/2017JE005426) and $10^{4-5} \text{ cm}^{-2}\text{s}^{-1}$ for GEOTAIL (Seki et al., 2001) observations. Peak energy fluxes of these ions observed by ARTEMIS are on the order of $10^{4-5} \text{ eV cm}^{-2}\text{str}^{-1}\text{s}^{-1}\text{eV}^{-1}$. Existing magnetospheric ion instruments are therefore capable of measuring the escaping ions even at L2.

1.4 Methodology

The basic mission of FATE can be accomplished by a spacecraft with fairly standard magnetospheric science instrumentation. Yet we must see the measured escaping fluxes in their spatial context in order to be able to associate them with the different escape routes. This is particularly important in transient situations when the flux increases by the arrival of a CIR, a CME, or a SEP event.

To obtain the 2D distribution, a multi-point observation approach is envisaged. This has been demonstrated for the near-Earth tail by several Cluster studies. At L2, where one can assume the gradients along the tail axis to be essentially zero, simultaneous measurements in 3 non-collinear points are sufficient to establish the 2D spatial structure and the time dependence. With one additional assumption (time stationarity, orientation of the plasma sheet) and/or statistical method, only 2 points are needed. To this end, FATE foresees 2 sub-spacecraft that relay their data through the main spacecraft. Since the goal is to localize the measurements in the 2D tail cross-section, these sub-spacecraft do not require advanced instrumentation and can be quite modest.

1.5. Required observations and strawman payload

1.5.1. Escaping ions and solar wind (main spacecraft)

* Ionospheric atomic ions (N^+ , O^+), molecular ions (N_2^+ , NO^+ , O_2^+), plasmaspheric He^+ from plasmaspheric energy up to solar wind velocity for

CIRs $\sim 800 \text{ km/s}$ (0.02-120 keV for O_2^+ , 0.02-60 keV for O^+ , 0.02-15 keV for He^+ , 0.02-8 keV/q for He^{++} , and 0.02-4 keV for H^+). These ion instruments must have sufficient G-factors to easily detect O^+ with $10^{4-8} \text{ cm}^{-2}\text{str}^{-1}\text{s}^{-1}\text{keV}^{-1}$, with expected flux of $10^{7-10} \text{ cm}^{-2}\text{s}^{-1}$ ($=1-100 \text{ cm}^{-3} * 10^{7-8} \text{ cm/s}$) for H^+ , and $10^{4-8} \text{ cm}^{-2}\text{s}^{-1}$ ($=0.001-1 \text{ cm}^{-3} * 10^{7-8} \text{ cm/s}$) for O^+ and N_2^+ or O_2^+ , in a narrow energy band.

$\Rightarrow 10^{5-9} \text{ keV cm}^{-2}\text{str}^{-1}\text{s}^{-1}\text{keV}^{-1}$ for H^+ and $10^{4-8} \text{ cm}^{-2}\text{str}^{-1}\text{s}^{-1}\text{keV}^{-1}$ with O/H ratio of 0.03-3%

\Rightarrow Required G-factor of $10^{-4} \text{ cm}^{-2}\text{s}$ for H^+ and $10^{-3} \text{ cm}^{-2}\text{s}$ for O^+ (and N_2^+ , O_2^+).

To achieve this requirement in an optimum way, we divide the task into three instruments:

(A1) Ion-1 (Micro-Channel Plate, MCP type): Mass separation is mandatory up to 40 keV.

(A2) Ion-2 (Solid State Detector, SSD type or MCP type): Covering up to $>60 \text{ keV}$ with a good energy resolution (to keep high and common G-factors for different species, we do not require mass resolution).

(A3) Ion-3 (SSD type): Ions 30-150 keV with mass separation (H^+ , He^{++} , O^+ , N_2^+/O_2^+) with some energy resolution.

* Tailward extent of the cold ion populations in the plasma sheet. If the density of such cold ions is high, the isotope ratio can be used to estimate the source altitude of escaping ions above the homopause.

(B) Cold ion mass spectrometer that can obtain isotope ratios.

1.5.2. Necessary support information (main spacecraft)

* Method to identify different regions of the deep-tail magnetosphere, e.g., magnetopause and plasma sheet boundary. This requires the approximate direction of magnetic (B) field. B-field is also needed to know the pitch angles. In addition, plasma parameters such as plasma density (n) are needed.

(C) MAG: B-field $\Rightarrow -64 \text{ nT}$ to $+64 \text{ nT}$ with 2 nT/0.1 Hz accuracy may work.

(D) LP: Langmuir Probe \Rightarrow a 15 m wire boom is sufficient for the main spacecraft even in the tenuous plasma in the lobe while a $< 1 \text{ m}$ boom is sufficient for the sub-spacecraft because of the spacecraft size.

* Method to estimate the magnetic connectivity to the near-Earth environment such as bi-directional electrons (20 eV-30 keV) and low frequency wave activity, and also to estimate the deformation of the escape routes. They are also helpful in distinguishing local acceleration of ions from escaped ions that travelled long distance.

(E) ELS: Electron energy spectrometer (20 eV - 30 keV).

(F) WAVE: Frequency analyzer for on-board calculations of data products (C) and (D).

* SEP monitor (MeV-range solar energetic particles) to give correct estimate at Earth by comparing with Sun-Earth L1 monitor from space weather programs (e.g., by ESA SSA SWE and NOAA).

(G) EP: MeV-range energetic particles (MeV ions, with option MeV/hundreds keV electrons).

1.5.3. Support information from the sub-spacecraft (6U cubesat form factor)

* Can detect solar wind and heavy ions with solar wind velocity up to 800 km/s. We again divide the task among two instruments.

(S1) Ions 0.1-15 keV with $\Delta E/E < 30\%$

(S2) Ions 15-120 keV with $\Delta E/E < 50\%$

* Method to identify different regions of the tail magnetosphere (either S3 or S4 is required).

(S3) B, i.e., the same as (C) with 0.7-2m boom.

(S4=TBD) n, i.e., the same as (D) with ≤ 1 m boom.

1.5.4. Measurements under discussion

* Monitoring of the exosphere (geocorona), which provides the seed population of outflowing ions. However, this information might become available from other space projects, and we might skip it in that case.

(H) UV imager to monitor the geocorona from emission/scattering of lines of neutral H, O, and N₂. Weekly information is sufficient.

1.6. Expected outcome with prescribed orbit and observations (including main aim)

FATE aims at answering the question "***What is the non-thermal ion escape rate from Earth as a function of solar, solar wind, and magnetospheric conditions?***" This comprises the sub-questions

(Q1) *What are the total escape fluxes of the principal ions?*

Q1a: *What are local fluxes of different ions?*

Q1b: *How large is the effective size of the relevant regions of escape?*

(Q2) *How does the plasma escape respond to transients, including CIRs, CMEs and SEPs?*

Q2a: *What is the response to normal solar wind variability?*

Q2b: *What is the effect of major transients?*

(Q3) *What is the relative importance of the different ion escape routes?*

Q3a: *What are the contributions of the direct, leaky, and indirect escape routes?*

Q3b: *What is the relation to the upper atmospheric conditions?*

Q3c: *How far do cold ions reach out into the far tail plasma sheet?*

FATE measurements can also contribute to extra questions, not directly related to ion escape:

(ex1) *How do plasma boundaries evolve nonlinearly?*

We expect nonlinear development of boundary waves, plasma mixing, and developed forms of turbulence, given the long plasma travel time from the Earth to L2.

(ex2) *What is the feedback of the magnetosphere-solar wind interaction on solar wind structures such as CIRs and CMEs?* This could be examined by a systematic L1-L2 comparison, which has not yet been done in the past.

(ex3) *Can measurements at L2, together with those at L1 and in geosynchronous orbit, provide more insight in the source and propagation pathway of SEP?* This could be relevant for space weather purposes.

Table 1 relates all these questions to the proposed instrument suite. Note that Q1b can to some extent be addressed with a single spacecraft by combining modeling and statistics, and we can accomplish a large part of the science even if both sub-spacecraft fail. The redundancy in case of failure of instruments is given in the last column. These "backup" methods also imply that instrument cross-calibration is possible, for instance for density (A1, A2, B, D, E) or energy flux density (A1, A2, A3).

Table 1. Measurement requirements versus science questions. Essential (+), Supportive (Δ)

| | Q1 | | Q2 | | Q3 | | | bonus | | | backup |
|-------------------|----------|----------|----------|----------|----------|----------|----------|----------|----------|----------|------------------------|
| | a | b | a | b | a | b | c | ex1 | ex2 | ex3 | |
| (A1) Ion 1 (MCP) | + | + | + | + | + | + | Δ | + | + | Δ | (A2), (B), (S) |
| (A2) Ion 2 | + | Δ | + | + | + | + | Δ | Δ | + | Δ | (A1), (S) |
| (A3) Ion 3 (SSD) | + | Δ | + | + | + | + | | + | | Δ | (A2), (G) |
| (B) cold ion mass | Δ | Δ | + | + | + | + | + | + | | | (A1) |
| (C) MAG + boom | Δ | Δ | + | Δ | + | | | + | | + | (D), (S) |
| (D) LP + boom | Δ | Δ | + | Δ | + | | Δ | + | | | (A1), (B), (E) |
| (E) ELS | Δ | Δ | + | Δ | + | | Δ | + | Δ | Δ | (D), (A1) |
| (F) WAVE | Δ | Δ | Δ | Δ | Δ | | | + | | | (C), (D) |
| (G) EP | | | Δ | + | | | | Δ | Δ | + | (A3) |
| (S) sub-S/C | Δ | + | Δ | Δ | Δ | Δ | Δ | + | Δ | | the other sub-S/C |
| (H) UVI | | | | Δ | | o | | Δ | | | ground-based/other S/C |

2. Mission configuration

2.1. Mission profile and communication for sub-spacecraft

2.1.1. Orbit

The trajectory of the main spacecraft must cover the 2D tail cross-section in order to obtain the 2D distribution statistically. The radial distance from the Sun-Earth line to be covered is less than $80 R_E$. In addition, inter-spacecraft distances between the main spacecraft (with propulsion) and the free-flying sub-spacecraft (without propulsion) must vary to obtain instantaneous gradients at varying spatial scales (occasionally $> 80 R_E$). This requires the sub-spacecraft to be placed at a semi-stable Lissajous/Halo orbit and the main spacecraft to take slightly different orbit that requires ΔV , as illustrated on the cover page, such that it catches up with the sub-spacecraft every 1-2 months.

In this strategy (a) the semi-axis of the sub-spacecraft's orbit in the north-south direction must be $80-120 R_E$ to include the plasma mantle, and (b) the main spacecraft must have enough propulsion for many small ΔV maneuvers. In this manner, the main spacecraft can control the inter-spacecraft distance from close distance (for sufficient telemetry to downlink from the sub-spacecraft to the main spacecraft) to $> 70 R_E$ (500,000 km). This method enables both a formation-flight configuration near the boundary and a large area of coverage for the rest of the time.

A Lissajous orbit with large semi-axis (initial velocity relative to the L2 point will be order of 50-100 m/s) is preferable, but it can also be a Halo orbit, depending on the insertion of the main spacecraft that depends on the requirements for the PLATO/ARIEL mission. Inserting the sub-spacecraft into the Lissajous orbit will be achieved by separating it when the main spacecraft is moving nearly along the Lissajous/Halo orbit with a deployment velocity on the order of only cm/s. The optimum deployment point will be the northernmost or southernmost location of the Lissajous/Halo orbit to optimize the initial location of the constellation near the plasma boundary with the most complicated structure near L2. Considering the short nominal operation time (3-6 months), the acceptable deployment error is of the order of 0.1 m/s and therefore the sub-spacecraft can safely stay within the region of study.

The deployment of the sub-spacecraft from the main spacecraft must not destabilize the spacecraft attitude. The deployment of both sub-spacecraft can be either simultaneously or at different times. Because of the small deployment velocity compared to the orbital velocity, simultaneous deployment makes the sub-spacecraft follow slightly different orbits, allowing a triangle constellation for a long period. However,

deployment at different times is optimum for better 2D coverage. The deployment timing will be decided based on updated models during the Phase-A study.

2.1.2. Communication

The required large inter-spacecraft distance may prohibit inter-spacecraft telecommunication during a long period. Therefore, the main spacecraft will download the data from sub-spacecraft only when the main spacecraft approaches the sub-spacecraft every 1-2 month. This method requires:

- (a) Method and subsystem that allows ranging of the sub-spacecraft from the Earth or the main spacecraft with < 100 km accuracy.
- (b) Subsystem (e.g., transponder) to navigate the main spacecraft closer to the sub-spacecraft close enough to allow high inter-spacecraft telemetry rate that decreases with r^{-2} .
- (c) Memory in the sub-spacecraft and scheme to transfer the downloaded data to the ground via the main spacecraft.

With 3.5U (10cm×10cm×35cm) for S/C bus, miniaturized technologies for all these tasks are available (for cubesats; qualification for operation at L2 remains to be demonstrated). For example, the sub-spacecraft with such S/C bus can communicate through the main spacecraft with the ground, through which ranging is possible. Since the trajectory of free-flying sub-spacecraft along the Lissajous/Halo orbit can approximately be predicted, ranging does not have to occur very often (in worst case once a month) to know the sub-spacecraft location with 100 km accuracy, which is the distance that the inter-spacecraft communication becomes \sim Mbps. A low-cost subsystem to control the distance even to < 1 km also exists.

2.2. Payload mass and power

Including all key payloads including booms, total science payload mass/power will be 36-39 kg/65-70 W (43-47 kg/78-84 W with margin) for the main spacecraft, and the mass for two sub-spacecraft with their payloads will be 20 kg (24 kg with margin) for 6U. Adding these two, the baseline science payload mass is 56-59kg (67-71 kg with margin). If we have to add the undecided payloads, the total science payload mass/power will be 63-66 kg/85-90 W (76-79 kg/102-108 W with margin).

Total mass is within 80 kg even in the heaviest estimate, but power might be a problem if we include undecided payloads. In that case, we share the power between different payloads by switching off observations that do not have to operate continuously. On the other hand, the main spacecraft and the sub-spacecraft are always sunlit because the Lissajous/Halo orbit does not approach the L2 saddle

point (Figure 1) that is in eclipse. Since the sub-spacecraft have attitude control (possible with 3.5U S/C bus out of 6U), the power provision for the sub-spacecraft is guaranteed.

In addition to science payloads, the main spacecraft must have extra subsystems related to formation flight.

* Deployers of the sub-spacecraft

* Main spacecraft subsystem to control the inter-spacecraft distance (e.g., transponder)

* Data handling system that transfers the data from the sub-spacecraft to the ground.

The associated mass (including margin) will not exceed 13 kg including margin for 6U sub-spacecraft.

Table 2. Summary of mass and power including DPU and PSU, and TRL level of the proposed science payload

| Payload to measure escaping ions | | | |
|--|--------------|--|--------------|
| 5 kg | 8 W | MIMS (TOF type hot ion up to 40 keV with $\Delta M/M > 10$), | TRL=5 |
| 4 kg | 8 W | Ion energy spectrometer with larger diameter (up to >60 keV without mass) | TRL>6 |
| 4 kg | 9 W | SSD Heavy ion detector for O^+ up to 140 keV | TRL \geq 4 |
| 5 kg | 12 W | Cold ion mass spectrometer | TRL \geq 6 |
| 2 kg | 4 W | DPU for particle (just add data from different payload and send to spacecraft) | TRL>6 |
| 20 kg | 41 W | (24 kg/49 W with 20% margin) | |
| Necessary support payload for main spacecraft | | | |
| 5 kg | 4 W | MAG-M (fluxgate magnetometer with a 5 m boom) | TRL>6 |
| 4 kg | 6 W | LP-M (Langmuir probe with a 15m boom) | TRL \geq 6 |
| 4 kg | 8 W | Electron energy spectrometer (hot electron for 0.02-30 keV) | TRL \geq 6 |
| 1-4 kg | 3-8 W | WAVE (wave analyser) | TRL \geq 5 |
| 2 kg | <3 W | EP (MeV-range energetic particle) | TRL \geq 4 |
| 16-19 kg | 24-29 | (19-23 kg/29-35 W with 20% margin) | |
| Sub-spacecraft (6U cubesat form factor x 2) with 3-4 payload | | | |
| < 8 kg | | 3.5U S/C bus | TRL \geq 4 |
| 0.7 kg | 4 W | 1U SWIM (TOF type hot ion up to 15 keV with $\Delta M/M > 2$) | TRL \geq 6 |
| 0.5 kg | <1 W | 0.5U Thin dead-layer SSD ion detector with range 15-120 keV (undecided) | TRL>6 |
| 0.7 kg | 2 W | 0.5U MAG-C with short (0.7-2m) boom | TRL>6 |
| <1.0 kg | <5 W | 0.5U LP-C with short (<1m) boom (undecided) | TRL \geq 4 |
| 10-11 kg x 2 | | (12-13 kg x 2 with margin) | |
| Undecided payload | | | |
| 5 kg | 20 W | UVI (to monitor geocorona) | TRL \geq 6 |
| 5 kg | 20 W | (6 kg/24 W with margin) | |

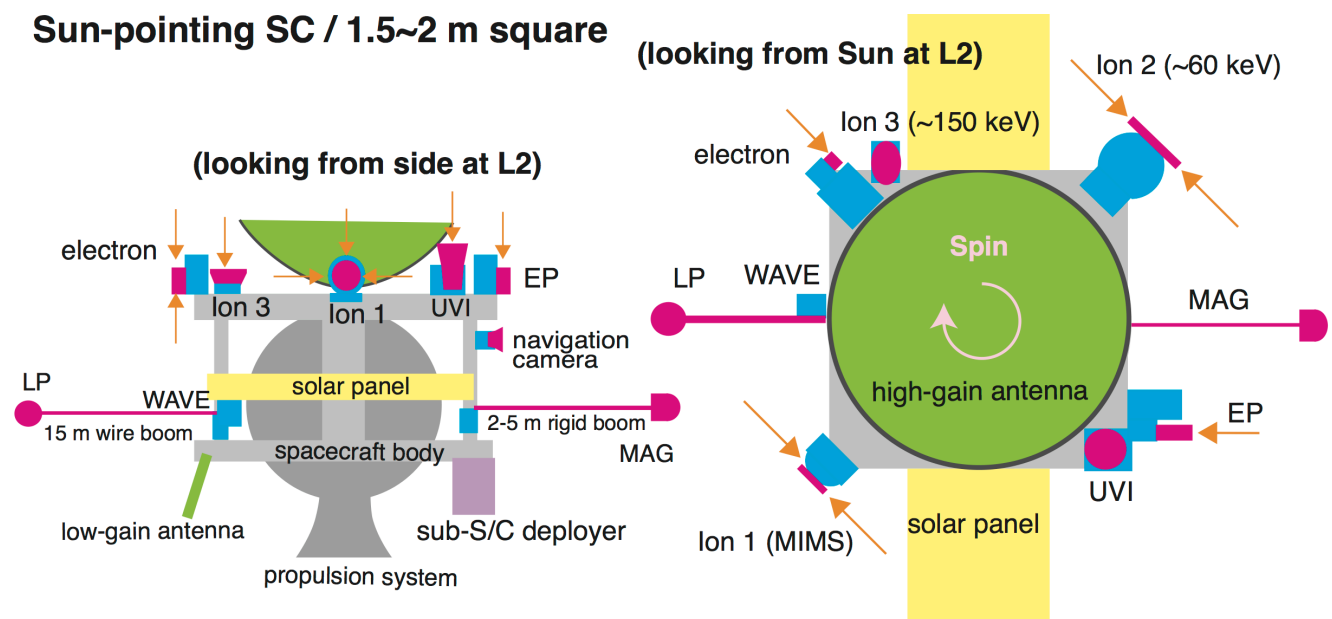


Figure 2: Accommodation of proposed science payloads and antennas.

2.3. Main Spacecraft provided by ESA

Possible accommodation of the science payloads and antennas is illustrated in Figure 2.

- (1) Spinning platform with 20-60 s spin period is used to make in-situ plasma measurements easier.
- (2) The spin axis of the main spacecraft point either toward Earth (with UVI) or to the Sun (without UVI) with 5° accuracy. If the spin is looking toward Earth, the offset angle from the solar wind direction varies up to 20° when the spacecraft explores up to $80 R_E$ from the Sun-Earth line (at $\sim 240 R_E$ downstream).
- (3) For many minor ΔV maneuvers to control inter-spacecraft distance to free-flying sub-spacecraft, electric propulsion can be used as an option.
- (4) The spacecraft has both high-gain (parabola or phased-array) antenna and low-gain antenna for redundancy.
- (5) The high-gain antenna must be large enough to allow direct download of the sub-spacecraft data (stored over 1-2 months) to the ground when the main spacecraft relays the data.
- (6) All particle instruments must have clear field of view (FOV) along the spin axis over more than 30° (the above-mentioned offset value of 20° plus moderate offset between the ion flow direction from the Sun direction), such that they can detect ions flowing in the solar wind direction during a spin.
- (7) The particle instruments should be oriented in the way that they can cover as wide FOV as possible during a spin. For example, the top-hat type instrument must have its symmetry axis perpendicular to the spin axis.
- (8) Solar panel, booms, and the sub-spacecraft deployer will be placed at the lower part of the spacecraft such that they will not affect incoming particles from upstream (Earth) side or photons coming from the Earth's exosphere.
- (9) The sub-spacecraft deployer should be mounted such that the spacecraft attitude will not be destabilized after the deployment of the sub-spacecraft.
- (10) In addition to the solar panels looking toward the Earth as illustrated to Figure 2, some solar panel will look toward the other directions in case of loss of attitude control.
- (11) The wire boom for LP will be provided by co-PI while solid boom for MAG will be provided by ESA.
- (12) EMC requirement is similar to Venus Express level if we have 5 m boom for MAG. This might even be shorter. Exact requirement is TBD.

With these conditions, the dry mass is expected to be less than 500 kg including instrument and margin, and we hence fuel mass can be as much as > 200 kg.

2.4. Sub-spacecraft provided by the team (outside ESA budget)

For the sub-spacecraft for multi-point measurements, we use two 6U cubesat form factor spacecraft (not necessarily with COTS components).

- (1) Both sub-spacecraft are identical, with the same payloads and same interface/telemetry specifications.
- (2) They are provided by Aalto U in Finland (as seen from ESA), and thus they are treated as a science payload. The actual manufacture will be divided among U Tokyo and Aalto U for the sub-spacecraft bus, with LTU for the sub-spacecraft-related subsystems in the main spacecraft.
- (3) Since sub-spacecraft data are transferred only every 1-2 month, each must have sufficient memory while the data volume from the instruments must remain limited.
- (4) The sub-spacecraft are 3-axis stabilized with attitude control. This is needed for both observation (particle FOV must look Sunward) and communication, and is possible at L2 (without the geomagnetic field).
- (5) The design of the deployer of the sub-spacecraft, located on the main spacecraft, is directly linked to the sub-spacecraft, and therefore falls under the responsibility of the sub-spacecraft consortium.

2.5. Attitude control

The accuracy requirement for attitude is 5° for the main spacecraft and 15° for the sub-spacecraft pointing to the Sun (solar wind) direction. Considering the spacecraft's motion along the XZ plane of $<5 R_E/\text{week}$ (which is $<1^\circ/\text{week}$ looking from $240 R_E$ distance) and the rotation around the Sun ($1^\circ/\text{day}$), the maximum change of the attitude relative to Earth is $8^\circ/\text{week}$ (from -4° to $+4^\circ$). Therefore, 5° accuracy can be achieved by the attitude reorientation once a week. An attitude knowledge of 0.5° for the main spacecraft and 3° for the sub-spacecraft is amply sufficient.

2.6. Radiation environment

We consider 4 radiation effects: (1) Outer surface charging due to the solar wind plasma and/or magnetotail, (2) Radiation damage from energetic particles for SEP, Galactic Cosmic Rays (GCR), and Jovian high-energy electrons, (3) Single-event upsets and bit flips, mostly due to GCRs, and (4) Deep dielectric discharges, mostly due to energetic electrons. As long as some countermeasures are foreseen against surface charging and deep dielectric charging, risks are relatively small. The cumulative radiation dose can be kept under control through the use of shielding (3 mm Al, ~ 2 krad/6 months). Single event upsets and bit flips that are caused by the energetic nature of the GCRs, Jovian electrons, and the

high peak fluxes of SEP events rates are limited (~1/day from Herschel experience).

2.7. Avoiding space debris

Since L2 is an unstable Lagrange point and the semi-stable orbits around L2 cover a very large area, the risk of the spacecraft becoming space debris is very small. Yet, to make sure that the free-flying sub-spacecraft will not remain in L2, we adjust the deployment angle of the sub-spacecraft such that the distance from L2 increases with time so that they are ejected into interplanetary space, but slow enough compared to the mission duration.

3. Management and collaboration

3.1. Spacecraft and Consortia

ESA's role will be generally limited to the main spacecraft. This includes all industry work and operation (MOC and SOC). Since individual payloads are small, we make consortia like the other plasma packages of the ESA planetary missions such as Rosetta/RPC, MEX-VEX/ASPERA, and JUICE/PEP-RPWI. For the FATE mission, we plan to have 3 consortia (Particle, Field, and Sub-spacecraft) plus one possible optical payload (UVI), as summarized in page 2. This means that the member states are responsible for the sub-spacecraft as a consortium, and ESA sees the sub-spacecraft only during occasional ranging (once a month) to determine its orbit with 100 km accuracy.

3.2. Data handling and archiving

ESA is responsible for the level 0 (telemetry) data distribution and archiving. ESA is also responsible for producing the summary plots of the telemetry data in the format specified by the science study team (SST). Once level 0 is distributed, co-PI teams are responsible for producing the level 1 (raw-readable format) and level 2 (cleaned and calibrated) data, and converting the level 2 data in a common format. The archived level 2 data for all spacecraft is owned by ESA for open use to everybody.

Before the level 2 archiving, which may take some years, co-PIs are responsible for making data open to the public for key information even at low level (like level 1 data) within 1 year. The information to be open is defined by ESA. For example particle data are likely published in the energy-time spectrogram format as well as integrated values (moment values).

3.3. International collaboration

We have payload-level international collaborations, as summarized in page 2. Collaboration with Japan is for sub-spacecraft and UVI instrument, for both of which all technology needed for the FATE mission is already available at U. Tokyo. Collaboration with USA is for the EP instrument sub-system from U. New Hampshire, and the second ion instrument for sub-spacecraft from SSL, which is the only institute that has experience with the thin dead layer detectors that can detect O^+ as low as 15 keV with SSD technology.

For the financial scheme, the official responsibility in securing the consortium/payload is Aalto U. for the sub-spacecraft and LATMOS for UVI. The available funding from JAXA is sufficient for their contribution. NASA normally offers support equivalent to a few instruments. Although the F-mission is relatively small in ESA's science program, the level of support needed from NASA is sufficient for the planned contributions. Collaboration with New Zealand (U. Auckland) is under discussion to provide a particle DPU through LTU. All science instruments will be funded by the relevant national agencies.

3.4. Nominal mission duration

To cover all conditions of dipole tilt and Earth's axis looking from L2, we need 3-6 months of continuous measurements depending on day of year when the operation starts. Also we expect many CIRs during 6 months and likely some CMEs. A 6-months observation period at the fixed L2 distance accumulates sufficient statistics.

If the resources allow, a prolonged observation is always useful in increasing the statistics, particularly for CIR and CME events. Also, we can examine usefulness of monitoring at L2 in addition to L1 for protecting space telescopes at L2 from severe space weather events, although that part of operation belongs to the SSA SWE program.

The mission design study can also consider repositioning the spacecraft after the nominal mission ends, e.g., to Mars L2 for studying ion escape at a non-magnetized planet, or sending it to a comet.

3.5. Cost

ESA is in charge of main spacecraft and a short boom (2-5 m) for MAG. If no other cost is included, the total cost will be about 145 Meur as summarized in the first row in Table 3. The cost for the national agencies will be 40-55 Meur for the science payload on the main spacecraft and 6-8 Meur for the two sub-spacecraft.

Table 3: Cost estimate for different options when the nominal operation is 6 months (+commissioning phase)

| Options | Project team | Industrial | Operation | Margin | Total |
|--|----------------|----------------|----------------|----------------|-----------------|
| S/C for L2 + a boom | 15 Meur | 95 Meur | 20 Meur | 15 Meur | 145 Meur |
| + deployer & communication for sub-S/C | | +5 Meur | | | 150 Meur |